

# Activation of STAT3 by the Hepatitis C Virus Core Protein Leads to Cellular Transformation

Takafumi Yoshida,<sup>1,2</sup> Toshikatsu Hanada,<sup>1</sup> Takeshi Tokuhisa,<sup>3</sup>  
Ken-ichiro Kosai,<sup>4</sup> Michio Sata,<sup>2</sup> Michinori Kohara,<sup>5</sup>  
and Akihiko Yoshimura<sup>1</sup>

<sup>1</sup>Division of Molecular and Cellular Immunology, Medical Institute of Bioregulation, Kyushu University, Maidashi, Higashi-ku, Fukuoka 812-8582, Japan

<sup>2</sup>Second Department of Internal Medicine, Faculty of Medicine, Kurume University, Kurume 830-0011, Japan

<sup>3</sup>Department of Developmental Genetics (H2), Graduate School of Medicine, Chiba University, Chuo-ku, Chiba 260-8670, Japan

<sup>4</sup>Department of Medical Science of Regeneration of the Cardiovascular System, Gifu University School of Medicine, Gifu 500-8705, Japan

<sup>5</sup>Department of Microbiology and Cell Biology, The Tokyo Metropolitan Institute of Medical Science, Honkomagome, Bunkyo-ku, Tokyo 113, Japan

## Abstract

The signal transducer and activator of transcription (STAT) family proteins are transcription factors critical in mediating cytokine signaling. Among them, STAT3 is often constitutively phosphorylated and activated in human cancers and in transformed cell lines and is implicated in tumorigenesis. However, cause of the persistent activation of STAT3 in human tumor cells is largely unknown. The hepatitis C virus (HCV) is a major etiological agent of non-A and non-B hepatitis, and chronic infection by HCV is associated with development of liver cirrhosis and hepatocellular carcinoma. HCV core protein is proposed to be responsible for the virus-induced transformation. We now report that HCV core protein directly interacts with and activates STAT3 through phosphorylation of the critical tyrosine residue. Activation of STAT3 by the HCV core in NIH-3T3 cells resulted in rapid proliferation and up-regulation of Bcl-XL and cyclin-D1. Additional expression of STAT3 in HCV core-expressing cells resulted in anchorage-independent growth and tumorigenesis. We propose that the HCV core protein cooperates with STAT3, which leads to cellular transformation.

Key words: STAT3 • phosphorylation • HCV • core protein • transformation

## Introduction

The signal transducer and activator of transcription (STAT)\* family proteins were identified in the last decade as transcription factors essential for mediating virtually all cytokine signaling (1, 2). These proteins become activated through tyrosine phosphorylation, which typically occurs through cytokine receptor-associated kinases, the Janus kinase (JAK) family proteins (3). In addition to their central

roles in normal cell signaling, recent studies have demonstrated that constitutively activated STAT signaling, especially STAT3, directly contributes to oncogenesis (4). For example, all *src* transformed cell lines exhibit constitutively activated Stat3 (5), and dominant-negative Stat3 suppresses *src* transformation without having any effect on *ras* transformation (6, 7). More directly, Bromberg et al. (8) demonstrated that a constitutively activated form of STAT3, STAT3-C, which has two substituted cysteine residues within the COOH-terminal loop of the SH2 domain, resulting in a spontaneous transcriptionally active dimer, causes cellular transformation scored by colony formation in soft agar and tumor formation in nude mice. Thus, the activated Stat3 molecule by itself can mediate cellular transformation. Extensive surveys of primary tumors and cell lines derived from tumors have indicated that an inappro-

Address correspondence to Akihiko Yoshimura, Division of Molecular and Cellular Immunology, Medical Institute of Bioregulation, Kyushu University Maidashi, Higashi-ku, Fukuoka 812-8582, Japan. Phone: 81-92-642-6823; Fax: 81-92-642-6825; E-mail: yakihiko@bioreg.kyushu-u.ac.jp

\*Abbreviations used in this paper: DEN, diethylnitrosamine; HBV, hepatitis B virus; HCC, hepatocellular carcinoma; HCV, hepatitis C virus; JAK, Janus kinase; LIF, leukemia-inhibitory factor; MOI, multiplicity of infection; NF, nuclear factor; PCNA, proliferating cell nuclear antigen; STAT, signal transducer and activator of transcription; Tg, transgenic.

appropriate activation of STAT3 occurs at a surprisingly high frequency in a wide variety of human cancers (9). However, mutations in the STAT3 gene have not been identified in these cancers, hence it remained to be determined how endogenous STAT3 is constitutively activated.

The hepatitis C virus (HCV), a major etiological agent of non-A and non-B hepatitis, leads to chronic infection and ultimately to liver cirrhosis and hepatocellular carcinoma (HCC; references 10 and 11). Globally, there are 0.25–1.2 million new cases of HCC annually, hence HCV is one of the major infectious causes of morbidity and mortality worldwide (12). HCV is a positive-strand RNA virus that consists of an ~9,600 base, and the open reading frame genome encodes a polyprotein of 3,010 amino acids, processed by cellular and viral proteases into three to four putative structural (core, E1, E2/p7) and at least six nonstructural (NS2, NS3, NS4A, NS4B, NS5A, NS5B) proteins. Among these, the HCV core protein derived from the NH<sub>2</sub>-terminal 191 amino acids of the precursor polyprotein has been implicated in cellular transformation. This was demonstrated in one transgenic (Tg) mouse line expressing the core protein in liver, which induce HCC (13), although this has been highly debated and there are several HCV core-Tg mouse lines that do not develop HCC. The transforming potential of the core itself has been shown to be weak; the core protein can transform fibroblastic cells in collaboration with other oncogenes, such as Ras. Therefore, it has been suggested that additional factors may be necessary for induction of cellular transformation by the HCV core. Kato and coworkers demonstrated that among HCV and hepatitis B virus (HBV) structural and nonstructural proteins, HCV core protein is the most potent signal inducer determined by using various reporter assays with the cAMP response element, the serum response element (SRE), and elements containing binding sites for nuclear factor (NF)- $\kappa$ B, activator protein 1 (AP-1), and serum response factor (SRF; reference 14). The HCV core protein also affects several transcription factor activities including LZIP and Elk-1; however, the role of these transcription regulators in core-mediated transformation is unclear (15, 16).

We now report that the HCV core protein interacts directly with STAT3 and selectively activates it. Activation of STAT3 by the HCV core in NIH-3T3 cells resulted in STAT3-dependent rapid proliferation and up-regulation of Bcl-XL and cyclin-D1. The core protein can also transform NIH-3T3 cells in collaboration with additional expression of wild-type STAT3. These data suggest that the constitutive activation of STAT3 plays an important role in transformation by the HCV core protein.

## Materials and Methods

**Core-Tg Mice and Carcinogen Treatment.** The Tg mouse was generated using a construct carrying HCV-core cDNA (HCV-1b strain) fused to the promoter of the HBV X gene (Px) (pPx-core; reference 17). Tg mice were developed using the conventional methods. (C57BL/6  $\times$  DBA/2) F1 mice were used to obtain fertilized eggs, and those founder mice were mated with C57BL/6

mice for over five generations. Expression of HCV core protein has been published (17). The core protein was expressed in various tissues including brain, heart, lung, kidney, thymus, and liver. However, protein levels in the liver were about one third of those in the spleen and other tissues.

4-wk-old male mice were given a single injection (intraperitoneal) of diethylnitrosamine (DEN; Sigma-Aldrich) at 10  $\mu$ g/g of body weight as described (18). 2 d later, these mice were killed, and portions of three liver lobes were used for immunoblotting and immunohistochemical studies. For immunoblotting, liver extracts were prepared by homogenizing tissue in extraction buffer (50 mM HEPES, pH 7.5, 150 mM NaCl, 1% NP-40, 1 mM EDTA, 1 mM vanadate). The protein concentration of each liver extract was determined using the DC Protein assay system (Bio-Rad Laboratories) according to manufacturer's directions. Subsequent immunoblot analysis was done using 20  $\mu$ g of total liver protein as described below.

Immunohistochemical detection of cyclin D1 and proliferating cell nuclear antigen (PCNA) was performed using formalin-fixed, deparaffinized mouse liver tissue sections and anti-PCNA and anti-cyclin D1 antibodies (Santa Cruz Biotechnology, Inc.), as described (18). Antibody-protein complexes were visualized using SAB kit (Dako) and 3,3'-diaminobenzidine according to the manufacturer's directions.

**Core and HCV cDNA.** The HCV core region (573 nucleotides) was also amplified by RT-PCR, using HCV RNA as a template extracted from the serum of a patient with chronic hepatitis C, genotype 1b. The nucleotide sequence is 98% and amino acid sequence is 100% identical to those of HCV strain MD7-1 (19). The cDNA was subcloned into expression vector pcDNA3 with the NH<sub>2</sub>-terminal Myc tag (six repeats; reference 20) (pcDNA3-Myc-core) or Flag-tagged vector (pCMV2-flag; Kodak; pFlag-core). This clone was used for most of the experiments in this study. Another core cDNA genotype 1b (21) was subcloned into the pEF1 vector (pEF-core; Invitrogen). Full-genome HCV cDNA was also cloned from the serum of a chronic hepatitis patient and subcloned into the Cre/loxP conditional expression cassette (pCALN) using a neo-resistant gene with poly A signal as a stuffer (21). For this study, the Cre/loxP cassette was removed by digestion with XhoI. Expression of all HCV proteins, including the core, E1, E2, NS1, NS2, NS3, NS4A, NS4B, NS5A, and NS5B were confirmed by Western blotting (unpublished data). Details on the construction of this plasmid will be published elsewhere.

**Cells and Transfection.** HepG2 cells and NIH 3T3 cells were cultured in DMEM containing 10% FCS and 10% calf serum (CS), respectively. Transient transfections of expression into HepG2 cells and NIH 3T3 were done using TransFast (Promega) or Fugene 6 transfection reagents (Roche). The transfection efficiency for HepG2 cells was 50–70%. An APRE-luciferase reporter gene for STAT3 activity (20) and a reporter gene construct containing IFN $\alpha$ -responsive ISRE (IFN-stimulating factor responsive element)-luciferase for IFN-stimulated gene factor 3 were as described previously (22). Luciferase assays were done using the dual-luciferase reporter system (Promega). cDNA for v-src in pcDNA3 was provided by Dr. Hamanaka (Nagoya University, Japan). The expression plasmid of Flag-tagged STAT3-C in pRC-CMV was provided by Dr. Darnell, Jr., The Rockefeller University, New York, NY (8). To create Flag-tagged wild-type STAT3, STAT3-C was replaced with WT-STAT3 cDNA.

**Retrovirus Construction and Infection.** The myc-tagged core cDNA was subcloned into a bicistronic retrovirus vector, pMX-IRES-EGFP (enhanced green fluorescent protein; reference 23).

A retrovirus was produced by transient transfection of a PLAT-E packaging cell line (24). 48 h after transfection, the culture supernatant was harvested, and NIH-3T3 cells ( $2 \times 10^5$  cells) were infected with appropriately diluted PLAT-E supernatant with 10  $\mu\text{g}/\text{ml}$  polybrene for 24 h. 100% infection was confirmed by EGFP fluorescence. Infected cells were expanded for 2–5 d, then immediately used for proliferation and colony-formation assays.

**Adenovirus.** Adenoviral vectors containing the genes for lacZ (Ad-lacZ), Myc-tagged SOCS3 (Ad-SOCS3), and HA-tagged Y705F-STAT3 (Ad-dnSTAT3) were prepared via homologous recombination in 293 cells as described (25). The viral preparations were titrated with a plaque-forming assay on 293 cells. The number of virus particles (measured in PFU) per cell was expressed as multiplicity of infection (MOI). The adenovirus was inoculated at MOI = 50, and 100% of the cells were infected, as assessed by lacZ staining. The cells were used for experiments immediately after infection.

**Transformation Assay.** 4–6-wk-old athymic, Balb-c/nu/nu mice were injected with  $10^6$  cells from various cell lines in 0.2 ml PBS. After 3 wk, the tumors were measured. Each cell line was tested in 2–3 different mice.

**Binding Assay.** Full-length core cDNA was ligated into a pGEX-4T vector to create the GST-fused core protein (GST-core). HepG2 cell extracts stimulated either with or without leukemia-inhibitory factor (LIF) were incubated with beads containing the GST or GST-core for 1 h at 4°C. After extensive washing, proteins bound to the beads were eluted by boiling in an SDS-sample buffer and immunoblotted with anti-STAT3, anti-ERK2, anti-NF- $\kappa\text{B}$  p65 subunit, or anti-GST antibodies (Santa Cruz Biotechnology, Inc.). A series of NH<sub>2</sub>-terminal and COOH-terminal deletion mutants of STAT3 and the core were generated by PCR and subcloned into pcDNA3-myc or pCMV2-flag vectors. These cDNAs were transiently expressed in 293 cells (1  $\mu\text{g}$  plasmid/transfection) and cell extracts were immunoprecipitated with either anti-Myc polyclonal antibody (Santa Cruz Biotechnology, Inc.) or anti-flag (M2; Eastman Kodak Co.), then analyzed by immunoblotting with anti-Myc (9E10) or anti-Flag antibodies.

**Immunoprecipitation and Western Blot Analysis.** Cells were lysed in the lysis buffer (50 mM HEPES pH 7.5, 150 mM NaCl, 0.5% NP-40, 1 mM EDTA, 1 mM vanadate, 1 mM DTT, 0.1 mM APMSF) and centrifuged at 12,000  $g$  for 10 min. Before the precipitation experiments, BSA were added at final concentrations 1 mg/ml, then, the supernatants were incubated with the indicated antibodies at 4°C for 1 h. Immune-complexes were precipitated with protein A-Sepharose (Amersham Biosciences). After washing three times with lysis buffer, the immunoprecipitates were resolved with SDS-PAGE and immunoblotted with the indicated antibodies as described (20). Nuclear and cytoplasmic extracts were prepared as described (8). Briefly, cells were scraped off the dish and pelleted; 3 $\times$  the pellet volume of cytoplasmic buffer was added (20 mM HEPES, pH 7.9, 10 mM KCl, 0.1 mM NaVanadate, 1 mM EDTA, 10% glycerol, 1 mM DTT, 1 mM PMSF), then left on ice for 10 min. The sample was lysed using a dounce homogenizer (10–20 strokes) and spun in an Eppendorf centrifuge for 5 min. The supernatant is the cytoplasmic fraction. The pellet was washed once with cytoplasmic buffer, then resuspended in 2 $\times$  the pellet volume with nuclear buffer (420 mM NaCl, 20% glycerol, 20 mM HEPES, pH 7.9, 10 mM KCl, 1 mM EDTA, 0.1 mM NaVanadate, 1 mM PMSF, 1 mM DTT). 10  $\mu\text{g}$  of each sample was used for immunoblotting with anti-STAT3 antibody. Anti-HCV core monoclonal antibody was purchased from Arista Biological Inc. Anti-JAK2 was purchased

from UBI; anti-tyrosine-phosphorylated STAT1, anti-tyrosine-phosphorylated STAT3, anti-tyrosine-phosphorylated STAT5, and anti-tyrosine-phosphorylated STAT6 were from Cell Signaling Technology; anti-tyrosine-phosphorylated JAK1 and JAK2 was from Quality Controlled Biochemicals, Inc.; anti-STAT1, anti-STAT3, anti-STAT5, anti-ERK2, anti-cyclin-D1, anti-bcl-X, anti-NF- $\kappa\text{B}$  p65 subunit, and anti-GST were from Santa Cruz Biotechnology, Inc.

## Results

**The HCV-Core Protein Induces Activation of STAT3.** It has been shown that a Tg expression of the HCV core protein in mice resulted in HCC in one case (13). We also developed HCV core Tg mice (Px-core Tg), in which the core protein is expressed ubiquitously (17). Malignant tumors (6 out of 22) developed in the skin and muscle of Px-core Tg mice up to 13 mo of age, whereas no tumors developed in their nontransgenic littermates. No HCC developed in our Tg mice, maybe because of relatively low levels of expression of the core protein in the liver. Similarly, it has been shown that Tg mice harboring the HBV X protein have only minor histopathologic alterations of the liver. However, injection of DEN resulted in a twofold increase in the incidence of HCC in the Tg mice compared with wild-type littermates (26). The extent of hepatocellular proliferation, as measured by the detection of PCNA and by the incorporation of 5-bromo-2'-deoxyuridine, was approximately twofold higher in the HBV-X protein Tg livers than in the wild-type (18). Thus, we asked if HCV core protein also contributes to induction of a premalignant stage in the liver after treatment with DEN. As shown in a new Fig. 1 A, the number of cyclin D1 positive hepatocytes were  $\sim 1.5$  times higher than the wild-type littermates. Similar results were obtained for PCNA staining (unpublished data). These data strongly suggest that the HCV core associates with dysregulated proliferation, which may ultimately lead to cellular transformation.

As constitutive activation of STAT3 often occurs in human tumors and STAT3 activation correlates with proliferation and antiapoptosis (27), we determined if the HCV core protein would affect STAT3 activity in the liver of Px-core Tg mice. Immunoblotting with an anti-phosphorylated STAT3-specific antibody revealed that phosphorylation occurred in tyrosine 705 (Y705) of STAT3 in two independent Tg mice livers, an event critical for dimerization and DNA binding, but not so in nontransgenic littermates (Fig. 1 B, lanes 1–4). Next, we examined the effect of DEN on STAT3 activation in the liver. 2 d after DEN injection, liver extracts were prepared. Tyrosine phosphorylation of STAT3 was much stronger in DEN-treated livers of Tg mice than in wild-type mice (Fig. 1 B, lanes 5–8). As STAT5 was not phosphorylated in Tg and wild type mice (Fig. 1 B, lanes 9 and 10), these data suggest that the core protein specifically induces and enhances STAT3 activation.

As illustrated in Fig. 2, A and B, STAT3 transcription activity was significantly increased by transient expression



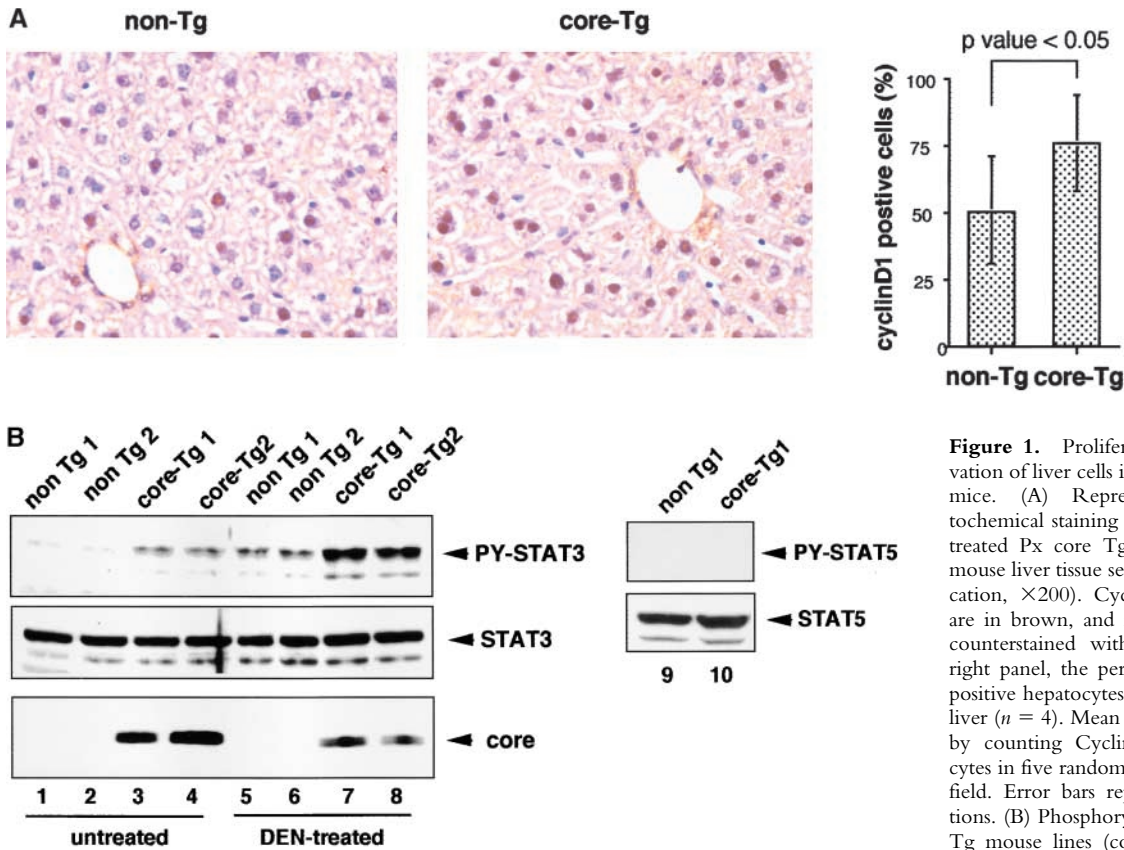


**Figure 1.** Proliferation and STAT3 activation of liver cells in HCV core protein Tg mice. (A) Representative immunohistochemical staining of Cyclin D1 in DEN-treated Px core Tg mouse and wild-type mouse liver tissue sections (original magnification,  $\times 200$ ). Cyclin D1-positive nuclei are in brown, and nonlabeled nuclei were counterstained with hematoxylin. In the right panel, the percentage of Cyclin D1-positive hepatocytes in DEN-treated mouse liver ( $n = 4$ ). Mean values were determined by counting Cyclin D1-positive hepatocytes in five random fields of  $\sim 250$  cells per field. Error bars represent standard deviations. (B) Phosphorylation of STAT3. Two Tg mouse lines (core-Tg1 and core-Tg2; lanes 3, 4, 7, 8, and 10) and their littermates

(non-Tg1 and non-Tg2; lanes 1, 2, 5, 6, and 9) were treated without (lanes 1–4, 9, 10) or with (lanes 5–8) DEN. 2 d later, liver cell extracts (20  $\mu$ g protein/lane) were prepared and immunoblotted with anti-phospho-STAT3 (PY-STAT3), STAT3, phospho-STAT5 (PY-STAT5), STAT5, and HCV core antibodies.

of the core protein in both HepG2 cells and NIH 3T3 cells, and STAT3 transcription activity by the core protein was further enhanced by LIF stimulation. In contrast, the HCV core protein did not affect interferon (IFN) $\alpha$ -induced reporter (ISRE-reporter) activity which reflects STAT1 and STAT2 activation (Fig. 2 C). Similar STAT3 activation by the core was observed in different cell types, including 293 cells and Hela cells (unpublished data). The core protein did not affect IFN $\gamma$ -induced STAT1 or EPO-induced STAT5 activation (unpublished data). Consistent with these findings, STAT3, but not STAT1 or STAT5, was significantly tyrosine-phosphorylated when the HCV core protein was expressed in HepG2 cells (Fig. 2 D, a, b, and c). STAT3 activation was observed by different core protein constructs derived from three independent HCV (genotype 1b) from different patients (Fig. 2 E, lanes 1–3). Expression of the full length HCV genome resulted in stronger STAT3 activation than did the core protein alone (Fig. 2 E, lane 4).

Interestingly, JAK1 as well as JAK2 was not activated by core-protein expression (Fig. 2 D, d and e). Furthermore, core-induced STAT3 phosphorylation was not blocked by AG490, a JAK inhibitor (Fig. 2 F, lanes 2 and 3), whereas AG490 efficiently blocked LIF-induced STAT3 activation (lanes 4 and 5). We have not examined Tyk2. However, it

is very unlikely that this kinase is involved, as SOCS3 adenovirus did not inhibit STAT3 activation by the core (see Fig. 5 D). These data indicate that the core protein activates STAT3 through cytokine receptor and JAK independent mechanisms.

**Direct Interaction between the Core and STAT3.** Activation of STAT3 by the core protein suggests a direct interaction between these two proteins. As shown in Fig. 3, STAT3 bound to the core both in vitro and in vivo. Both phosphorylated and nonphosphorylated forms of STAT3 bound to the GST-fused core protein in vitro (Fig. 3 A). We examined whether the core protein directly interacts with ERK2 (MAP kinase) or the NF- $\kappa$ B p65 subunit, as the core has been shown to activate MAP kinase and NF- $\kappa$ B under certain circumstances (14, 16). We observed no direct interaction of the core with these proteins in vitro (Fig. 3 A).

Next, we determined the region of STAT3 responsible for binding to the core. As shown in Fig. 3, B and C, binding experiments using truncated forms of STAT3 revealed the linker region of STAT3 to be essential for interaction with the core protein. For the core protein,  $\Delta$ C2 (1–113) bound and transactivated STAT3, whereas  $\Delta$ C3 (1–75) did not do so; thus residues 75–113 were important. Similarly,  $\Delta$ N2 (91–191) but not  $\Delta$ N3 (120–191)

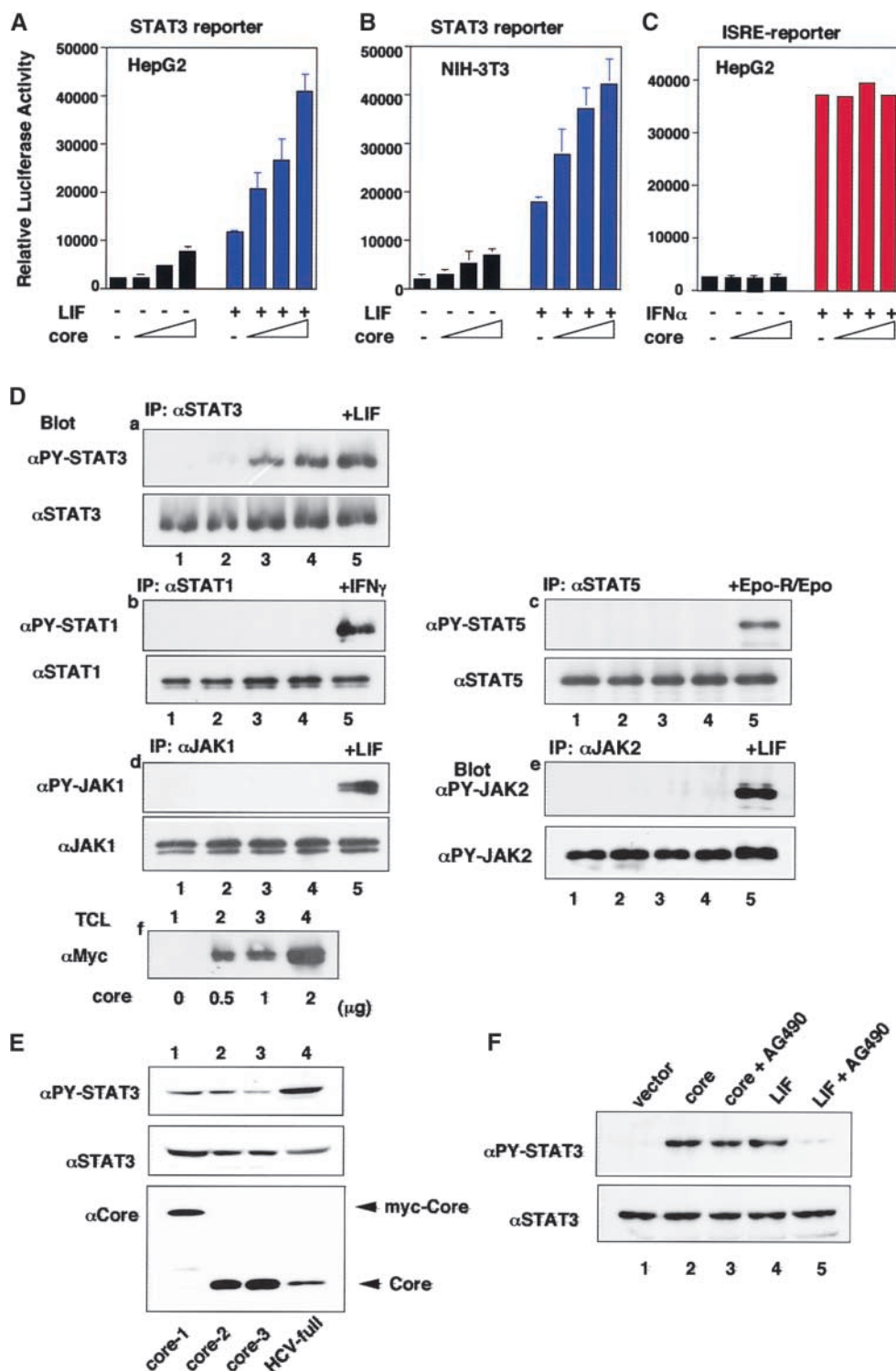


**Figure 2.** Activation of STAT3 by HCV core protein. (A–C) Reporter gene assay. HepG2 (A and C) or NIH-3T3 (B) cells were transfected with 0.5, 1, or 2  $\mu$ g plasmid of the pcDNA3-Myc-core and then stimulated by either 10 ng/ml LIF (A and B) or 100 ng/ml IFN $\alpha$  (C) for 6 h. STAT3- (A and B) or ISRE- (C) dependent luciferase activity was measured. (D) Phosphorylation of STAT3 by the core protein. HepG2 cells were transfected with 0 (lanes 1 and 5), 0.5 (lane 2), 1 (lane 3), 2 (lane 4)  $\mu$ g of the core plasmid, and STAT3 (a), STAT1 (b), STAT5 (c), JAK1 (d), and JAK2 (e) were then immunoprecipitated. The immunoprecipitates were blotted with anti-phosphorylated forms-specific antibodies. As a positive control (lanes 5), cells were stimulated with LIF or IFN $\gamma$  for STAT3, STAT1, and JAK1 phosphorylation. For STAT5, 293 cells transfected with the Erythropoietin (Epo) receptor (Epo-R) were stimulated with Epo. (E) Activation of STAT3 by three independent HCV core cDNAs and full-length HCV genomic DNA. pcDNA3-Myc-core (core-1, lane 1), pPx-core (core-2, lane 2), pEF-core (core-3, lane 3), and pCALN-HCV (HCV-full, lane 4) were transiently expressed in HepG2 cells then, total cell extracts were immunoblotted with indicated antibodies. (F) HepG2 cells transfected with empty vector pcDNA3-Myc (lane 1) or with pcDNA3-Myc-core (lanes 2 and 3) or untransfected cells (lanes 4 and 5) were treated without (lanes 1–3) or with (lanes 5 and 6) 10 ng/ml LIF for 3 h, then further incubated with (lanes 3 and 5) or without (lanes 1, 2, and 4) AG490 (50  $\mu$ M) for 6 h. Total cell extracts were immunoblotted with anti-PY-STAT3 or anti-STAT3 antibodies.

bound and activated STAT3; thus residues 91–120 were important. Based on these findings, amino acids 91–113 are essential not only for STAT3 binding but also for STAT3 transcriptional activation (Fig. 3, D–F). These data indicate that the core protein directly interacts with STAT3, which leads to tyrosine phosphorylation and the activation of STAT3.

The core protein locates mostly in the cytoplasm, but a significant fraction was also seen in the nucleus (28). A subcellular fractionation study indicates that small fraction of STAT3 was translocated to the nucleus in the presence of core protein (Fig. 4 A, lane 4). LIF induced translocation of STAT3 in the nucleus (lane 6), and nuclear localization of STAT3 was further enhanced in the presence of

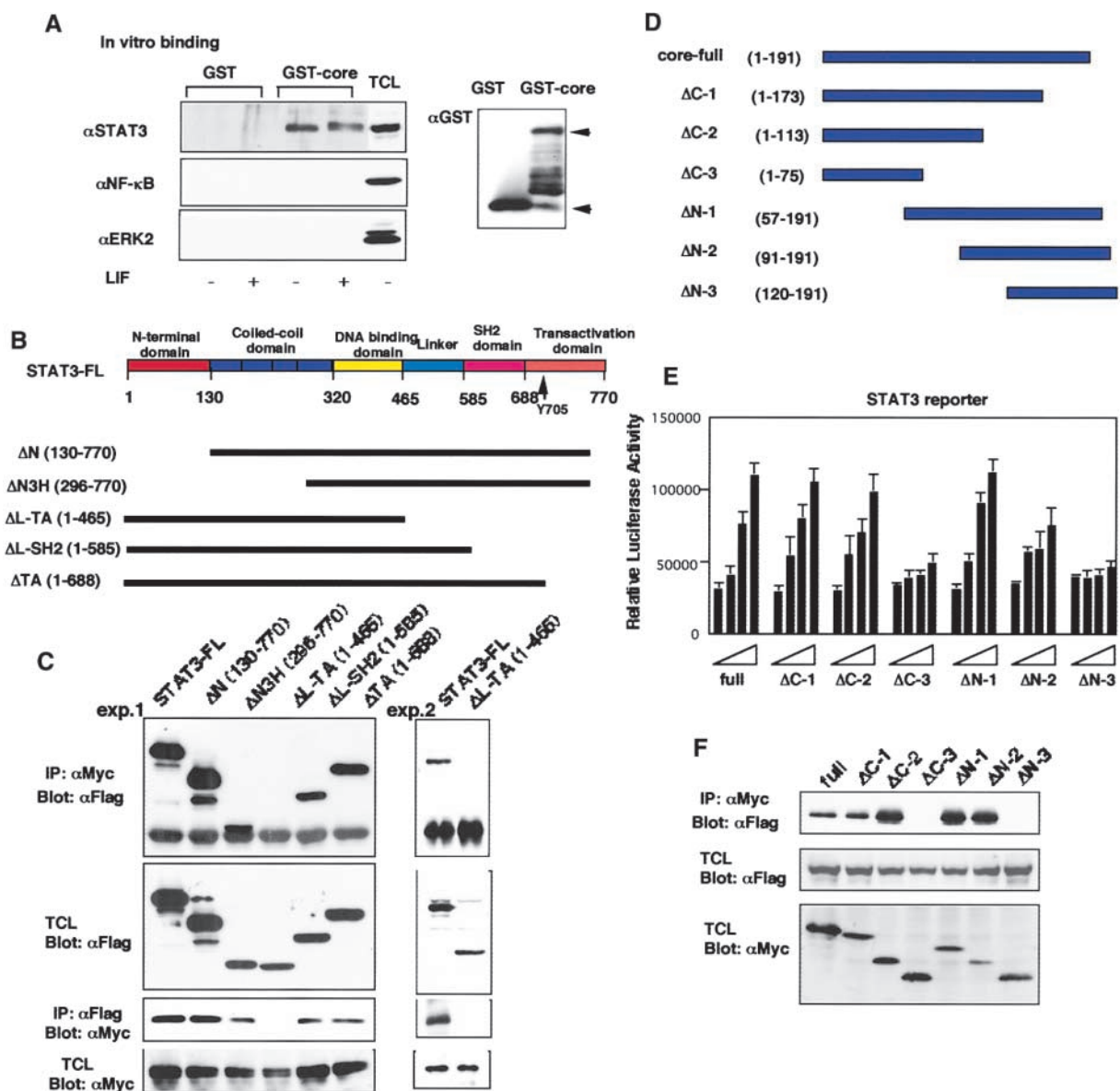


**Figure 3.** Interaction between the core protein and STAT3. (A) In vitro binding experiment. HepG2 cell extracts stimulated with (+) or without (–) LIF were incubated with either GST or GST-core bound to glutathione-Sepharose. Aliquots of total cell extracts (TCL) and proteins bound to the beads were immunoblotted with anti-STAT3, anti-NF-κB p65, and anti-ERK2 antibodies. Purified GST and GST-core fusion protein (0.1 μg protein) was also blotted with anti-GST. (B) Schematic diagrams of structural domains and deletion mutants of STAT3. (C) Flag-tagged STAT3 deletion mutants and the myc-tagged core were coexpressed in 293 cells and then immunoprecipitated with either anti-Myc or anti-Flag antibodies. The total cell extracts (TCL) or immunoprecipitates (IP) were blotted with anti-Myc or anti-Flag antibodies. To confirm the lack of binding between the core protein and ΔL-TA construct, data of a separate experiment are shown in the right (exp. 2). (D) Schematic diagrams of the deletion construct of the core protein. (E) HepG2 cells were transfected with an APRE-luciferase reporter gene and an increased amount of indicated core deletion mutants. After 24 h transfection, luciferase activity was measured. (F) The 293 cells were transfected with flag-tagged STAT3 and myc-tagged core deletion mutants. Immunoprecipitates with anti-Myc antibody or TCL were blotted with anti-Flag and anti-Myc antibodies.

the core protein (lane 8). We then examined the subcellular localization of the core and phosphorylated STAT3, using immunofluorescence microscopy. As expected, phosphorylated STAT3 colocalized with the core protein in HepG2 and NIH-3T3 cells (Fig. 4 B); mostly in the cytoplasm, but there was a small fraction in the nucleus. Treatment of cells with LIF accelerated translocation of STAT3 in the nucleus. However, a significant fraction of the phosphorylated STAT3 was still present in the cyto-

plasm in the core-transfected cells, while phosphorylated STAT3 was mostly present in the nucleus in nontransfected cells. Such cytoplasmic retention of phosphorylated STAT3 in the presence of the core protein also supports the notion of a strong interaction between STAT3 and the core protein.

Although the molecular mechanism of selective STAT3 phosphorylation by the core is not clear, we suspect that STAT3-core interaction may prevent dephosphorylation.



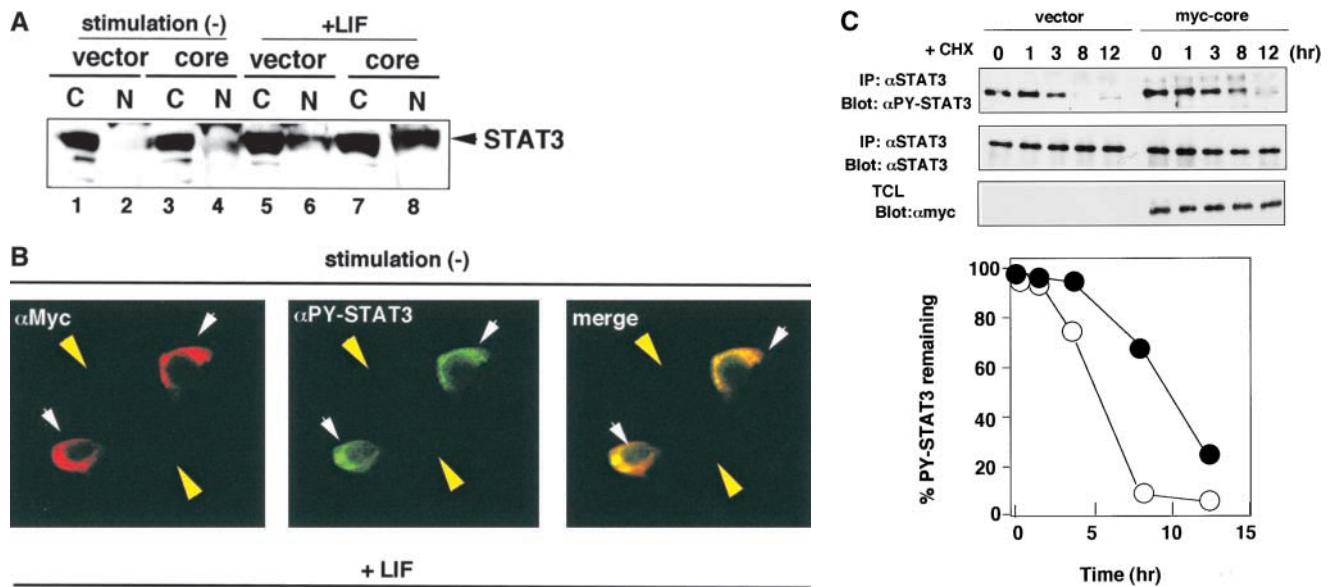


**Figure 4.** Nuclear localization of STAT3 (A and B) and time course of dephosphorylation of STAT3 (C). HepG2 cells transfected with empty vector (lanes 1, 2, 5, and 6) or pcDNA3-Myc-core (lanes 3, 4, 7, and 8) were stimulated without (lanes 1–4) or with (lanes 5–8) 10 ng/ml LIF for 30 min. Nuclear (N) and cytoplasmic (C) extracts (20  $\mu$ g each) were analyzed by immunoblotting with anti-STAT3 antibody. (B) HepG2 cells were transfected with Myc-tagged core cDNA and then immunostained with anti-myc (monoclonal; red) or anti-phosphorylated STAT3 (polyclonal; green) antibodies followed by incubation with FITC- and Cy3-conjugated secondary antibodies. White arrowheads indicate the position of core-transfected cells, and yellow arrowheads indicate nontransfected cells. Similar results were obtained by at least three independent experiments. (C) Time course of dephosphorylation. HepG2 cells transfected with or without the core cDNA (transfection efficiency was >60%) were stimulated with 10 ng/ml LIF for 30 min before cycloheximide (CHX) treatment. The cells were washed and incubated without LIF in the presence of 100  $\mu$ g/ml CHX for the indicated periods. The immunoprecipitates with anti-STAT3 antibody were analyzed by immunoblotting with the indicated antibodies. The levels of phosphorylated STAT3 in nontransfected (open circle) and transfected (closed circle) cells were quantitated by densitometry of the immunoblots using NIH Image software.

phorylated STAT3 (polyclonal; green) antibodies followed by incubation with FITC- and Cy3-conjugated secondary antibodies. White arrowheads indicate the position of core-transfected cells, and yellow arrowheads indicate nontransfected cells. Similar results were obtained by at least three independent experiments. (C) Time course of dephosphorylation. HepG2 cells transfected with or without the core cDNA (transfection efficiency was >60%) were stimulated with 10 ng/ml LIF for 30 min before cycloheximide (CHX) treatment. The cells were washed and incubated without LIF in the presence of 100  $\mu$ g/ml CHX for the indicated periods. The immunoprecipitates with anti-STAT3 antibody were analyzed by immunoblotting with the indicated antibodies. The levels of phosphorylated STAT3 in nontransfected (open circle) and transfected (closed circle) cells were quantitated by densitometry of the immunoblots using NIH Image software.

Thus, dephosphorylation of phosphorylated STAT3 was compared by incubating cells with a protein synthesis inhibitor cycloheximide. As shown in Fig. 4 C, phosphorylation of STAT3 was sustained by the core protein expression. This suggests that the HCV core protein either protects STAT3 from phosphatases or recruits unknown tyrosine kinase(s) to STAT3, thereby inducing the constitutive phosphorylation of STAT3.

*Core-induced Promotion of Proliferation Is Dependent on STAT3.* Next, we directed attention to the effect of HCV core protein on biological functions of STAT3. NIH-3T3 cells were infected with a retrovirus (pMX) carrying the core cDNA. As shown in Fig. 5 A, overexpression of the core resulted in an increased proliferation rate in NIH-3T3 cells, yet the core protein expression alone did not induce cellular transformation (see Fig. 6). Potent STAT3 phosphorylation was observed in NIH-3T3 transformants (NIH-3T3/core) expressing the core protein (Fig. 5 B). To examine the role of STAT3 on core-dependent hyperproliferation, NIH-3T3/core cells were further infected with adenovirus carrying lacZ (control), SOCS3, or Y705F-STAT3 (25; Fig. 3 C). Y705F-STAT3 has been

shown to function as a dominant negative form of STAT3 (dnSTAT3; reference 29). As dnSTAT3 can bind to the core (unpublished data), overexpression of dnSTAT3 sequesters the core protein from endogenous STAT3. On the other hand, SOCS3 binds to gp130 as well as to JAKs and inhibits JAK tyrosine kinase activity (30, 31). We confirmed that both SOCS3- and dnSTAT3-adenovirus infection completely inhibited LIF-induced STAT3 activation and IL-6-dependent proliferation of synovial cells from patients with rheumatoid arthritis, but did not affect proliferation of parental NIH-3T3 cells (25). As shown in Fig. 5, C and D, overexpression of dominant negative STAT3 reduced the growth rate of NIH-3T3/core cells to levels seen in parental NIH-3T3 cells, and diminished the phosphorylation of STAT3, whereas SOCS3 did not strongly affect growth rate or phosphorylation status. Similar growth suppression by dnSTAT3 was observed using HepG2 stable transformants expressing the core protein (unpublished data). These data confirmed that the growth-promoting activity of the core protein depends on STAT3 but core-mediated STAT3 activation is independent of the cytokine/JAK pathway.

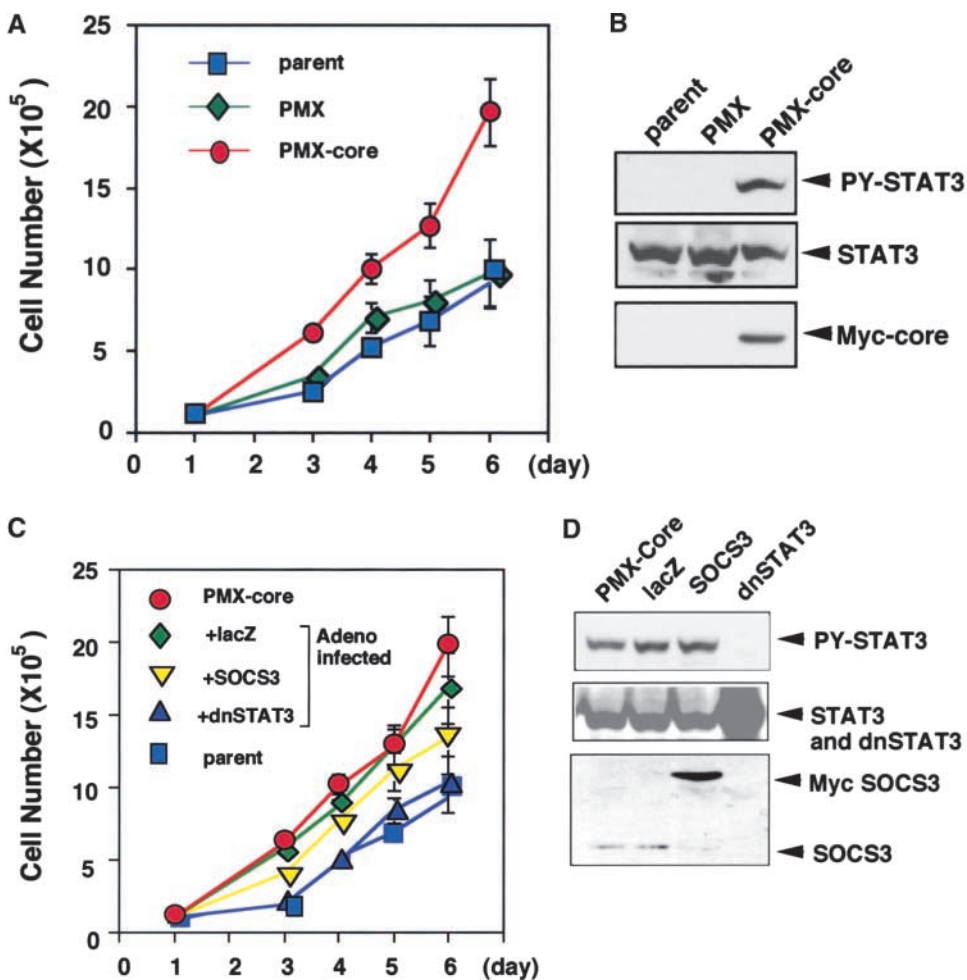


**Figure 5.** Effect of the HCV core on the proliferation of NIH-3T3 cells. (A) NIH-3T3 cells were infected with a retrovirus vector carrying the core (pMX-core) or control virus (pMX), then plated into 35 mm dishes and the cell number was counted daily under normal growth conditions. The mean cell number with standard error of triplicate experiments is shown. (B) Total cell extracts from parental NIH-3T3 cells (parent) or infected cells were immunoblotted with anti-phospho-STAT3 or anti-STAT3. (C) The NIH-3T3 cells infected with a pMX-core retrovirus vector (NIH-3T3/core) were further infected with adenovirus carrying lacZ, SOCS3, and Y705F-STAT3 (dnSTAT3) at MOI 50. After infection, the cells were plated and scored daily (triplicate experiments). (D) Total cell extracts of infected cells were blotted with anti-phospho-STAT3, anti-STAT3 or anti-SOCS3.

*Transformation by the Core Requires STAT3 Activation.* Next, we examined effects of core protein on cellular transformation. Recent studies suggested that STAT3 is necessary for the full transforming activity of *v-src* and that a constitutively activated form of STAT3 (STAT3-C) transformed normal fibroblasts (5–7). Thus, we examined the transforming potential of the core protein in combination with wild-type (WT)-STAT3 or STAT3-C. As shown in Table I and Fig. 6 A, expression of only the core (pMX-core) or transfection of the WT-STAT3 did not produce colonies in soft agar. However, transfection of WT-STAT3 into NIH-3T3 cells infected with the pMX-core did result in colony formation. The efficiency of colony formation and colony size by WT-STAT3 and the core (WT-STAT3/core) were comparable to those seen with STAT3-C (Fig. 6 A and Table I). The combination of the core and STAT3-C further increased colony formation efficiency (Table I). Cells were recovered from these transformed colonies and cultured. The levels of exogenous WT-STAT3 in these cells formed in soft agar were 1.5–2 times higher than endogenous STAT3 (Fig. 6 B), and both exogenous and endogenous STAT3 were tyrosine phosphorylated by the core (see Fig. 8). Therefore, the level of STAT3 is critical for transforma-

tion by the core protein. Requirement of further STAT3 expression for transformation in NIH-3T3 cells may be due to relatively low contents of STAT3 in this fibroblastic cell line compared with contents in the hepatocarcinoma cell line HepG2 and mouse liver tissues (Fig. 6 B, and unpublished data).

We then directly compared the plating efficiency in soft agar of newly established WT-STAT3/core transformed cell lines to that of STAT3-C transformed cells. The number of colonies formed per cell plated (plating efficiency) in WT-STAT3/core cells was comparable to that seen in STAT3-C (Table I). The colony-forming ability by WT-STAT3 and the core was significantly reduced by the dominant-negative STAT3 adenovirus but not by the SOCS3 virus (Fig. 6, A and B), thereby indicating that constitutive STAT3 activation plays an important role in colony-forming potential in soft agar.

Next, the tumorigenicity of cells transformed with wild-type STAT3 and the core was determined. When 10<sup>6</sup> cells from either of two WT-STAT3/core clones were injected subcutaneously into nude mice, tumors became apparent at the injection site within 2 to 4 wk. These tumors were as large as those of cells transformed with STAT3-C (Table II and Fig. 7 A). Hematoxylin and eosin staining of formalin-



**Table I.**

Colony formation assay		Plating efficiency of stable NIH-3T3-derived cell lines		
Vector	Colony number (SD)	Cell line	Inoculated cells	Colony number (SD)
pMX	0 (0)	NIH-3T3	10 <sup>6</sup>	0 (0)
pMX + WT-STAT3	0 (0)	NIH-3T3-core	10 <sup>6</sup>	0 (0)
pMX + STAT3-C	8 (4)	WT-STAT3	10 <sup>6</sup>	0 (0)
pMX-core	0 (0)	WT-STAT3/core	10 <sup>4</sup>	110 (32)
pMX-core + WT-STAT3	10 (4)	STAT3-C	10 <sup>4</sup>	92 (26)
pMX-core + STAT3-C	20 (10)	STAT3-C/core	10 <sup>4</sup>	222 (42)
<i>v-src</i>	96 (22)	<i>v-src</i>	10 <sup>3</sup>	180 (34)

NIH-3T3 cells were infected with pMX or pMX-core viruses and then transfected with WT-STAT3, STAT3-C, or *v-src*. Transfected cells (10<sup>6</sup>) were plated in soft agar. 3 wk later, the colony number was determined. Results shown are the mean  $\pm$  SD of 3–8 experiments. The plating efficiency of representative cell lines derived from soft agar or retrovirus infection (NIH-3T3-core) or clones selected in G418 (WT-STAT3) was determined by plating the indicated number of cells into soft agar and counting the colonies after 10 d.

fixed sections revealed that WT-STAT3/core-derived tumor cells had multiple nucleoli, large nuclei, and frequent mitoses (Fig. 7 B). The cells from Stat3-C-derived tumors were more spindle-like and appeared to be more organized than did cells from WT-STAT3/core- or *v-src*-derived tumors. WT-STAT3/core-derived tumor cells appeared to be more similar to *v-src*-derived tumors than did STAT3-

C-derived tumor cells (Fig. 7 B). Mice injected with parental NIH-3T3 cells or 3T3-core never developed tumors (Table II). Western blot analysis of extracts derived from STAT3/core-containing tumors revealed high levels of STAT3 and core protein, hence the growing tumor cells retained these two proteins (unpublished data). These results indicate that, by either core protein association or by

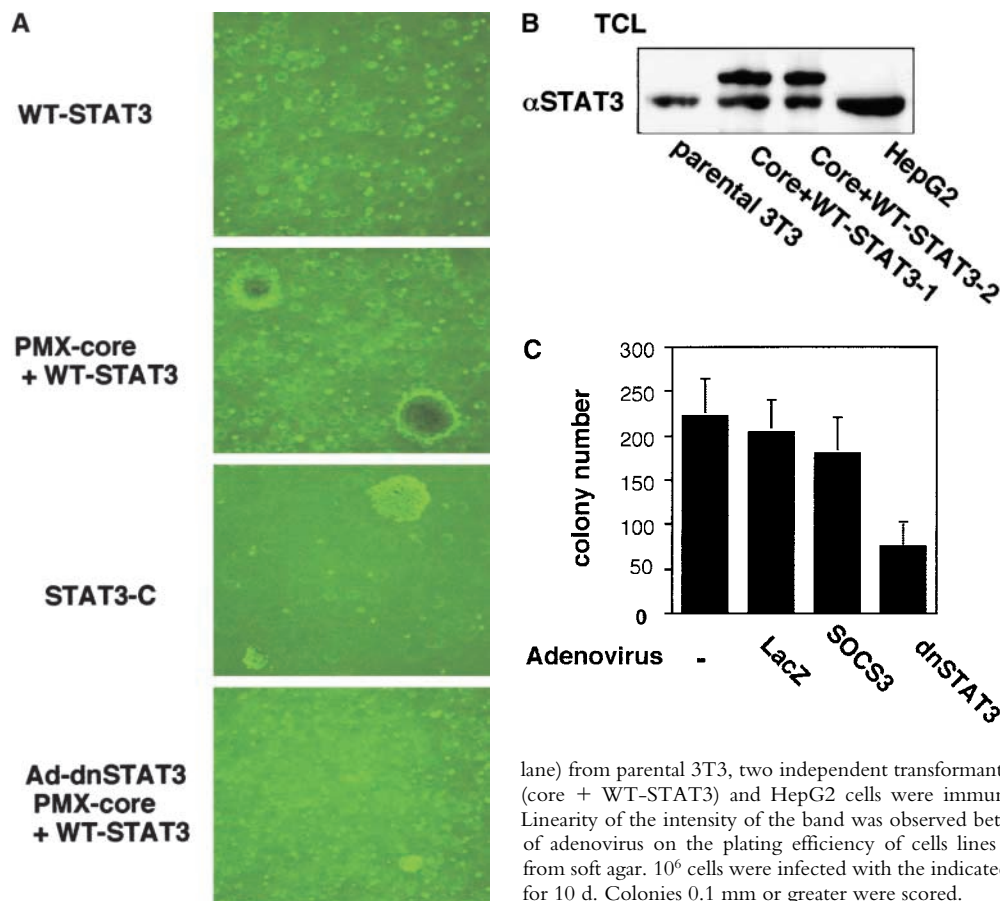


**Figure 6.** Transforming potential of WT-STAT3 and core-transfected cells. (A) NIH-3T3 cells or cells infected with the pMX-core were transfected with WT-STAT3 or STAT3-C and plated into soft agar and photographed on day 10. In the lowest panel, cells were infected with adenovirus carrying dnSTAT3 (Ad-dnSTAT3) at MOI = 50. (B) The levels of endogenous and exogenous STAT3 in NIH-3T3 and comparison with HepG2 cells. The same amount of cell extracts (15  $\mu$ g protein/lane) from parental 3T3, two independent transformants expressing the core and WT-STAT3 (core + WT-STAT3) and HepG2 cells were immunoblotted with anti-STAT3 antibody. Linearity of the intensity of the band was observed between 5–40  $\mu$ g protein. (C) The effect of adenovirus on the plating efficiency of cells lines expressing WT-STAT3/core derived from soft agar. 10<sup>6</sup> cells were infected with the indicated adenovirus (MOI = 50) and cultured for 10 d. Colonies 0.1 mm or greater were scored.

**Table II.** Tumors in Nude Mice

Cell line	Tumor size (cm)	cm <sup>3</sup>
NIH-3T3	ND	
NIH-3T3-core	ND	
WT-STAT3	ND	
WT-STAT3/core		
Clone 1	0.8 × 0.8 × 1.0	0.64
	0.4 × 0.5 × 0.8	0.16
	0.8 × 0.6 × 0.8	0.38
Clone 2	1.8 × 1.5 × 1.5	4.05
	1.6 × 1.2 × 1.2	2.34
	1.2 × 1.0 × 1.0	1.20
STAT3-C	1.2 × 0.8 × 1.0	0.96
	1.2 × 1.5 × 1.6	2.88
	1.8 × 1.2 × 1.0	2.16
<i>ν-src</i>	3.0 × 4.0 × 2.5	30.0

Cells (10<sup>6</sup>) from NIH-3T3, *ν-src*, STAT3-C, and WT-STAT3/core cell lines were injected into the flank of athymic nude mice. Each cell line was determined in 2–3 different mice. Tumor size was determined 3 wk after injection. ND, not detected.

point mutations, constitutively active STAT3 possesses similar oncogenic potential.

*Transcriptional Events Controlled by Core/Stat3 that may be Related to Transformation and Cell Growth.* To examine events downstream from the constitutively active STAT3/core or STAT3-C that promote tumorigenesis, we examined the expression of cyclin-D1 and Bcl-XL, which are involved in cell-cycle progression and antiapoptosis, respectively, and direct target genes of STAT3 (8). We also examined SOCS3, which is induced by STAT3 (32, 33). As shown in Fig. 8, there was a drastic increase in the concentration of cyclin D1 and Bcl-XL in cells transformed by STAT3-C, WT-STAT3/core, and *ν-src*. However, as non-transformed NIH-3T3/core cells also expressed high levels of cyclin D and Bcl-XL, these two STAT3 target genes may play an important role in rapid proliferation (Fig. 5), but are not sufficient for cellular transformation. It will be important to identify new STAT3 target genes directly involved in tumorigenesis.

We also observed the elevated expression of SOCS3 in cells expressing the core protein (Fig. 8). This is consistent with previous reports indicated that SOCS3 expression is regulated by STAT3. Previously, HCV genome expression was reported to inhibit interferon-STAT1 signaling by an unknown mechanism (34). Up-regulation of SOCS3 may be one mechanism involved in suppression of the IFN signaling pathway (35), which confers the interferon-resistance seen in HCV-infected cells.

## Discussion

During the past several years, data have accumulated indicating that human tumor samples contain constitutively activated STAT3. Artificially created gain-of-function mutant STAT3, STAT3-C, clearly demonstrated the tumorigenic potential of STAT3. To date, no active mutation has been found in STAT3 genes in human tumors. On the other hand, there is abundant descriptive evidence that links core protein to cellular transformation, but the mechanism was not clarified. In our work, we noted a strong link between HCV core protein and the constitutive activation of STAT3, events which lead to growth dysregulation. As our present study is overexpression system of one of the viral proteins using cell lines and a model mouse, we may not be able to simply apply our conclusion to the physiological infection conditions. Therefore, confirmation of our hypothesis by using human specimens infected with HCV is necessary in the future study. However, our study demonstrated that STAT3 activation by the HCV core protein is an important step for transformation in vitro. This will provide a new insight into the mechanism of HCC development and a new therapeutic target, i.e., STAT3.

As cells expressing the core alone were not tumorigenic, for the appearance of HCC, some secondary ‘hit(s)’, such as elevated expression of STAT3 or activation of ras (36), must be necessary for the development of a malignant phenotype. Up-regulation of cyclin D1 and Bcl-XL may explain the increase in growth rate by activation of STAT3, yet these two genes are not sufficient for cellular transformation. We are currently searching for genes specifically expressed in transformed cells by WT-STAT3/core but not in cells expressing the core or WT-STAT3 alone.

Yoshikawa and colleagues reported evidence that inactivation of SOCS1 by gene methylation and the consequent constitutive activation of cytokine-JAK/STAT (especially STAT3) signaling pathways are responsible for growth of HCCs (37). Their study as well as our data provide new insights into the role of STAT3 in HCC development. We also observed that colony formation of HepG2 cells in soft agar can be inhibited by dnSTAT3 adenovirus (unpublished data). These data strongly suggest that constitutive activation of STAT3 may play an important role in colony formation of HCC cells in soft agar. As core protein expression occurred only in the presence of HCV (HCV genome is not integrated into hepatocyte DNA), core/STAT3 interaction may be an initial step of STAT3 activation, then loss of SOCS-1 expression takes over the constitutive activation of STAT3. Thus, the constitutive activation of STAT3 induced by viral or cellular oncogenes, or loss of suppressors presents an attractive target for drug discovery with the potential of inducing cell death or inhibiting the growth of human HCV-mediated hepatocarcinomas. Our dominant negative STAT3 adenovirus or a minimal peptide that inhibits STAT3 signaling developed by Turkson et al. (38) could be useful as a lead for gene therapy or peptidomimetic drug design. Moreover, the

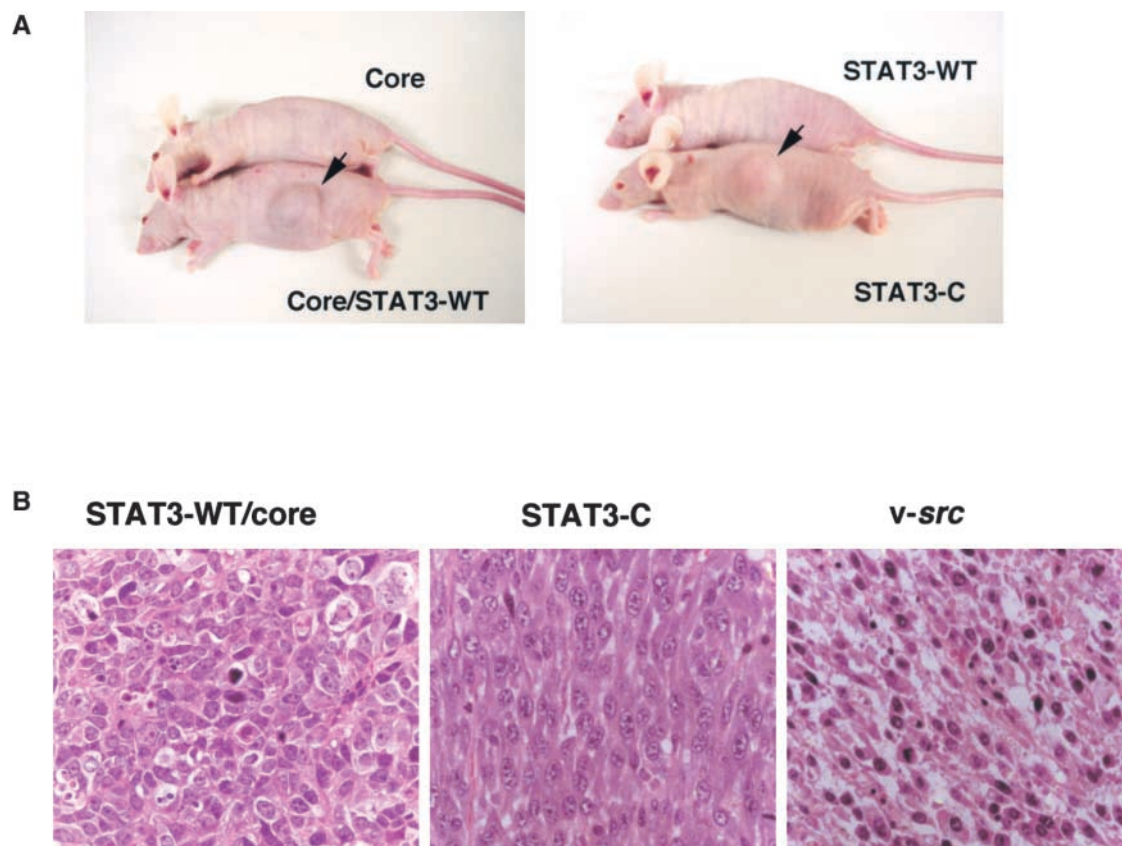
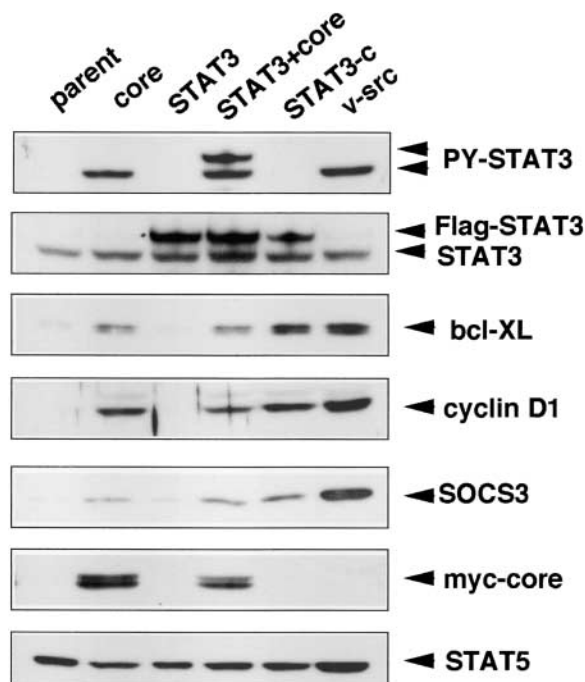


**Figure 7.** Tumorigenicity of cells transformed with WT-STAT3 and core-transfected cells. (A) WT-STAT3/core or STAT3-C transformed cell lines were injected into nude mice, and the mice were photographed 3 wk later. (B) Paraffin sections from WT-STAT3/core, STAT3-C and *v-src*-containing tumors were stained with hematoxylin and eosin and viewed at 400 $\times$  magnification.



present experiments provide the tools to pursue the basis of STAT3-mediated transformation, including a search of novel STAT3 target genes and heightened interest in the molecular mechanism of the constitutive activation of STAT3 seen in cancer. Also, other viral oncoproteins or cellular protooncogenes may cooperate with STAT3, thereby contributing to malignant transformation.

As the core protein has no tyrosine kinase activity, the manner in which it induces tyrosine phosphorylation of STAT-3 is not clear. Our experiments suggest that coexpression of the core resulted in a decrease in the dephosphorylation rate of phosphorylated STAT3 (Fig. 4 C). Thus, the core may prevent access of phosphatases to the STAT3, or the core recruits a tyrosine kinase to STAT3. However, we detected no tyrosine kinase activity in the immunoprecipitates with anti-core antibody. Therefore, we suspect that the former case is more likely. This may provide a novel approach to selectively regulate the activation of STAT3 without affecting other cytokine signaling pathways.

**Figure 8.** Cell extracts were prepared from parental NIH-3T3 cells (parent; lane 1), core-infected cells (core) (lane 2), and representative clones isolated from soft agar (STAT3 + core [lane 4], STAT3-C [lane 5], and *v-src* [lane 6]), and NIH-3T3 transformant expressing WT-STAT3 (lane 3), then immunoblotted with the indicated antibodies.



Although our pX-core Tg mice developed tumors in the skin and muscle, HCC was not evident in these Tg mice. Furthermore, HCV structural protein Tg mice developed spontaneous focal infiltration of lymphocytes, hepatocyte necrosis, degeneration, and altered foci with mitotic hepatocytes, but had no neoplastic or cancerous lesions in liver by the age of 20 mo (39). However, Lerat et al. reported that hepatocellular adenoma or carcinoma developed in older male Tg mice expressing RNA of the complete viral polyprotein in the liver (40). Therefore, a heterologous overexpression system of structural and nonstructural proteins may have stronger oncogenic potential than does the expression of individual viral proteins. In this context, it is interesting that whole HCV genome expression more strongly induced STAT3 phosphorylation as compared with the core protein alone (Fig. 2 E). Transcriptional activity of STAT3 was also more strongly upregulated by the full HCV genome than by the core alone (unpublished data). Therefore, STAT3 activation can also occur not only by core protein expression but also by expression of whole HCV proteins. Recently, a similar constitutive activation of STAT3 by the nonstructural HCV protein, NS5A has been noted (41). In this case, oxidative stress and intracellular  $Ca^{2+}$  was involved, since antioxidants or  $Ca^{2+}$  chelators eliminated the NS5A-induced activation of STAT3. In contrast, we observe no effects of these agents on core-mediated STAT3 activation (unpublished data), suggesting that STAT3 may be activated by multiple mechanisms and by different viral proteins. Further study is underway to define the relationship between STAT3 activation, transformation and full HCV protein expression.

We thank H. Ohgusu, Ms. M. Sasaki, and Ms. Y. Kawabata for excellent technical assistance, and M. Ohara for comments on the manuscript.

This work was supported in part by grants from the Ministry of Education, Science, Technology, Sports, and Culture of Japan, the Japan Health Science Foundation, the Human Frontier Science Program, Haraguchi Memorial Foundation for Cancer Research, and the Japan Research Foundation for Clinical Pharmacology.

Submitted: 24 December 2001

Revised: 27 June 2002

Accepted: 17 July 2002

## References

- Darnell, J.E., Jr. 1997. STATs and gene regulation. *Science*. 277:1630–1635.
- Stark, G.R., I.M. Kerr, B.R. Williams, R.H. Silverman, and R.D. Schreiber. 1998. How cells respond to interferons. *Annu. Rev. Biochem.* 67:227–264.
- Ihle, J.N. 1995. Cytokine receptor signaling. *Nature*. 377: 591–594.
- Bromberg, J.F., and J.E. Darnell, Jr. 2000. The role of STATs in transcriptional control and their impact on cellular function. *Oncogene*. 19:2468–2473.
- Yu, C.L., D. Meyer, G.S. Campbell, A.C. Lerner, C. Carter-Su, J. Schwartz, and R. Jove. 1995. Enhanced DNA-binding of a Stat3-related protein in cells transformed by the *src* oncoprotein. *Science*. 269:81–83.
- Bromberg, J.F., C.M. Horvath, D. Besser, W.W. Lathem, and J.E. Darnell, Jr. 1998. Stat3 activation is required for cellular transformation by *v-src*. *Mol. Cell. Biol.* 18:2553–2558.
- Turkson, J., T. Bowman, R. Garcia, E. Caldenhoven, R.P. De Groot, and R. Jove. 1998. Stat3 activation by *src* induces specific gene regulation and is required for cell transformation. *Mol. Cell. Biol.* 18:2545–2552.
- Bromberg, J.F., M.H. Wrzeszczynska, G. Devgan, Y. Zhao, R.G. Pestell, C. Albanese, and J.E. Darnell, Jr. 1999. Stat3 as an oncogene. *Cell*. 98:295–303.
- Bowman, T., R. Garcia, J. Turkson, and R. Jove. 2000. STATs in oncogenesis. *Oncogene*. 19:2474–2488.
- Aach, R.D., C.E. Stevens, F.B. Hollinger, J.M. Mosley, D.A. Peterson, P.E. Taylor, R.G. Johnson, L.H. Barbosa, and G.J. Nemo. 1991. Hepatitis C virus infection in post-transfusion hepatitis. An analysis with first- and second-generation assays. *N. Engl. J. Med.* 325:1325–1329.
- Saito, I., T. Miyamura, A. Ohbayashi, H. Harada, T. Katayama, S. Kikuchi, Y. Watanabe, S. Koi, M. Onji, Y. Ohta, et al. 1990. Hepatitis C virus infection is associated with the development of hepatocellular carcinoma. *Proc. Natl. Acad. Sci. USA*. 87:6547–6549.
- Idilman, R., N. De Maria, A. Colantoni, and D.H. Van Thiel. 1998. Pathogenesis of hepatitis B and hepatitis C-induced hepatocellular carcinoma. *J. Viral Hepat.* 5:285–299.
- Moriya, K., H. Fujie, Y. Shintani, H. Yotsuyanagi, T. Tsutsumi, K. Ishibashi, Y. Matsuura, S. Kimura, T. Miyamura, and K. Koike. 1998. The core protein of hepatitis C virus induces hepatocellular carcinoma in transgenic mice. *Nat. Med.* 4:1065–1067.
- Kato, N., H. Yoshida, S. Kioko Ono-Nita, J. Kato, T. Goto, M. Otsuka, K. Lan, K. Matsushima, Y. Shiratori, and M. Omata. 2000. Activation of intracellular signaling by hepatitis B and C viruses: C-viral core is the most potent signal inducer. *Hepatology*. 32:405–412.
- Jin, D.Y., H.L. Wang, Y. Zhou, A.C. Chun, K.V. Kibler, Y.D. Hou, H. Kung, and K.T. Jeang. 2000. Hepatitis C virus core protein-induced loss of LZIP function correlates with cellular transformation. *EMBO J.* 19:729–740.
- Hayashi, J., H. Aoki, K. Kajino, M. Moriyama, Y. Arakawa, and O. Hino. 2000. Hepatitis C virus core protein activates the MAPK/ERK cascade synergistically with tumor promoter TPA, but not with epidermal growth factor or transforming growth factor alpha. *Hepatology*. 32:958–961.
- Honda, A., M. Hatano, M. Kohara, Y. Arai, T. Hartatik, T. Moriyama, M. Imawari, K. Koike, O. Yokosuka, K. Shimotohno, and T. Tokuhisa. 2000. HCV-core protein accelerates recovery from the insensitivity of liver cells to Fas-mediated apoptosis induced by an injection of anti-Fas antibody in mice. *J. Hepatol.* 33:440–447.
- Madden, C.R., M.J. Finegold, and B.L. Slagle. 2001. Hepatitis B virus X protein acts as a tumor promoter in development of diethylnitrosamine-induced preneoplastic lesions. *J. Virol.* 75:3851–3858.
- Nagayama, K., M. Kurosaki, N. Enomoto, S. Maekawa, Y. Miyasaka, J. Tazawa, N. Izumi, F. Marumo, and C. Sato. 1999. Time-related changes in full-length hepatitis C virus and hepatitis activity. *J. Virol.* 263:244–253.
- Yasukawa, H., H. Misawa, H. Sakamoto, M. Masuhara, A. Sasaki, T. Wakioka, A. Ohtsuka, T. Imaizumi, T. Matsuda, J.N. Ihle, and A. Yoshimura. 1999. The JAK-binding protein JAB inhibits *Janus* tyrosine kinase activity through binding in

- the activation loop. *EMBO J.* 18:1309–1320.
21. Wakita, T., C. Taya, A. Katsume, J. Kato, H. Yonekawa, Y. Kanegae, I. Saito, Y. Hayashi, M. Koike, and M. Kohara. 1998. Efficient conditional transgene expression in hepatitis C virus cDNA transgenic mice mediated by the Cre/loxP system. *J. Biol. Chem.* 273:9001–9006.
  22. Yoneyama, M., W. Suhara, Y. Fukuhara, M. Sato, K. Ozato, and T. Fujita. 1996. Autocrine amplification of type I interferon gene expression mediated by interferon stimulated gene factor 3 (ISGF3). *J. Biochem.* 120:160–169.
  23. Nosaka, T., T. Kawashima, K. Misawa, K. Ikuta, A.L. Mui, and T. Kitamura. 1999. STAT5 as a molecular regulator of proliferation, differentiation and apoptosis in hematopoietic cells. *EMBO J.* 18:4754–4765.
  24. Morita, S., T. Kojima, and T. Kitamura. 2000. Plat-E: an efficient and stable system for transient packaging of retroviruses. *Gene Ther.* 7:1063–1066.
  25. Shouda, T., T. Yoshida, T. Hanada, T. Wakioka, M. Oishi, K. Miyoshi, S. Komiya, K. Kosai, Y. Hanakawa, K. Hashimoto, et al. 2001. Induction of a cytokine signal regulator, SOCS3/CIS3, as a new therapeutic strategy for the treatment of inflammatory arthritis. *J. Clin. Invest.* 108:1781–1788.
  26. Slagle, B.L., T.H. Lee, D. Medina, M.J. Finegold, and J.S. Butel. 1996. Increased sensitivity to the hepatocarcinogen diethylnitrosamine in transgenic mice carrying the hepatitis B virus X gene. *Mol. Carcinog.* 15:261–269.
  27. Hirano, T., K. Ishihara, and M. Hibi. 2000. Roles of STAT3 in mediating the cell growth, differentiation and survival signals relayed through the IL-6 family of cytokine receptors. *Oncogene.* 19:2548–2556.
  28. Chang, S.C., J.H. Yen, H.Y. Kang, M.H. Jang, and M.F. Chang. 1994. Nuclear localization signals in the core protein of hepatitis C virus. *Biochem. Biophys. Res. Commun.* 205:1284–1290.
  29. Nakajima, K., Y. Yamanaka, K. Nakae, H. Kojima, M. Ichiba, N. Kiuchi, T. Kitaoka, T. Fukada, M. Hibi, and M. Hirano. 1996. A central role for Stat3 In IL-6-induced regulation of growth and differentiation in M1 leukemia cells. *EMBO J.* 15:3651–3658.
  30. Schmitz, J., M., Weissenbach, S. Haan, P.C. Heinrich, F. Schaper. 2000. SOCS3 exerts its inhibitory function on interleukin-6 signal transduction through the SHP2 recruitment site of gp130. *J Biol. Chem.* 275:12848–12856.
  31. Nicholson, S.E., D. De Souza, L.J. Fabri, J. Corbin, T.A. Willson, J.G. Zhang, A. Silva, M. Asimakis, A. Farley, A.D. Nash, et al. 2000. Suppressor of cytokine signaling-3 preferentially binds to the SHP-2-binding site on the shared cytokine receptor subunit gp130. *Proc. Natl. Acad. Sci. USA.* 97:6493–6498.
  32. Auernhammer, C.J., C. Bousquet, and S. Melmed. 1999. Autoregulation of pituitary corticotroph SOCS-3 expression: characterization of the murine SOCS-3 promoter. *Proc. Natl. Acad. Sci. USA.* 96:6964–6969.
  33. Cassatella, M.A., S. Gasperini, C. Bovolenta, F. Calzetti, M. Vollebregt, P. Scapini, M. Marchi, R. Suzuki, A. Suzuki, and A. Yoshimura. 1999. Interleukin-10 (IL-10) selectively enhances CIS3/SOCS3 mRNA expression in human neutrophils: evidence for an IL-10-induced pathway that is independent of STAT protein activation. *Blood.* 94:2880–2889.
  34. Heim, M.H., D. Moradpour, and H.E. Blum. 1999. Expression of hepatitis C virus proteins inhibits signal transduction through the Jak-STAT pathway. *J. Virol.* 73:8469–8475.
  35. Song, M.M., and K. Shuai. 1998. The suppressor of cytokine signaling (SOCS) 1 and SOCS3 but not SOCS2 proteins inhibit interferon-mediated antiviral and antiproliferative activities. *J. Biol. Chem.* 273:35056–35062.
  36. Ray, R.B., L.M. Lagging, K. Meyer, and R. Ray. 1996. Hepatitis C virus core protein cooperates with ras and transforms primary rat embryo fibroblasts to tumorigenic phenotype. *J. Virol.* 70:4438–4443.
  37. Yoshikawa, H., K. Matsubara, G.S. Qian, P. Jackson, J.D. Groopman, J.E. Manning, C.C. Harris, and J.G. Herman. 2001. SOCS-1, a negative regulator of the JAK/STAT pathway, is silenced by methylation in human hepatocellular carcinoma and shows growth-suppression activity. *Nat. Genet.* 28:29–35.
  38. Turkson, J., D. Ryan, J.S. Kim, Y. Zhang, Z. Chen, E. Haura, A. Laudano, S. Sebt, A.D. Hamilton, and R. Jove. 2001. Phosphotyrosyl peptides block Stat3-mediated DNA binding activity, gene regulation, and cell transformation. *J. Biol. Chem.* 276:45443–45455.
  39. Honda, A., Y. Arai, N. Hirota, T. Sato, J. Ikegaki, T. Koizumi, M. Hatano, M. Kohara, T. Moriyama, M. Imawari, et al. 1999. Hepatitis C virus structural proteins induce liver cell injury in transgenic mice. *J. Med. Virol.* 59:281–289.
  40. Lerat, H., M. Honda, M.R. Beard, K. Loesch, J. Sun, Y. Yang, M. Okuda, R. Gosert, S.Y. Xiao, S.A. Weinman, and S.M. Lemon. 2002. Steatosis and liver cancer in transgenic mice expressing the structural and nonstructural proteins of hepatitis C virus. *Gastroenterology.* 122:352–365.
  41. Gong, G., G. Waris, R. Tanveer, and A. Siddiqui. 2001. Human hepatitis C virus NS5A protein alters intracellular calcium levels, induces oxidative stress, and activates STAT-3 and NF-kappa B. *Proc. Natl. Acad. Sci. USA.* 98:9599–9604.